# Statistical learning methods of knee joint vibroarthrographic signals for chondromalacia screening and diagnosis

JITKOMUT SONGSIRI
Department of Electrical Engineering
Chulalongkorn University

and

KAKANAND SRUNGBOONMEE
Center of Data Mining and Biomedical Informatics
Mahidol University

Research Project Number: ENG-59-012
Chula Engineering Research Support Grant
Faculty of Engineering
Chulalongkorn University
Bangkok
August 2560

# Statistical learning methods of knee joint vibroarthrographic signals for chondromalacia screening and diagnosis

Jitkomut Songsiri, Ph.D.
University of California, Los Angeles

and

Kakanand Srungboonmee, Ph.D.
Marquette University

Research Project Number: ENG-59-012
Chula Engineering Research Support Grant
Faculty of Engineering
Chulalongkorn University

**Abstract**

Patellar resurfacing during total knee arthroplasty (TKA) depends on surgeon's decisions and has been discussed if resurfacing is better than non-resurfacing. This paper aims to discuss the similarities and differences of the vibroartrographic (VAG) signal of the knee underwent TKA with either resurfaced or non-resurfaced patella in time-frequency domain. Motion trends and noises were filtered and then processed with Ensemble Empirical Model Decomposition (EEMD) and Detrended Fluctuation Analysis (DFA), which decomposes a non-stationary signal into a set of modes and discards modes that are uncorrelated. However, time-frequency analysis of processed signals suggests no significant differences between both classes and the results rather depend on the individual knee condition.

# Acknowledgement

We wish to thank Satit Thiengwittayaporn, MD, Department of Orthopaedics Surgery, Bangkok Metropolitan Administration Medical College and Vajira Hospital for the data sets. We thank Tanut Aranchayanont for preparing codes to analyze the signals. This research is financially supported by the Chula Engineering Research grant.

# Contents

# List of Figures



# List of Tables

# 1 Introduction

To diagnose the knee pathology, physicians rely on physical exam of the knee before confirmation with medical imaging techniques such as x-ray or MRI. Vibroarthrographic (VAG) signal is the vibration signal of the joint, recorded from an accelerometer. When the joint has changed its lubrication state or articular cartilage surface roughness, the signal can alter [CGZ78]. VAG signal has been found as a potential to be used as a diagnostic tool, in addition to the physical exam, in detection of the knee pathology [WKR10, LLL+14]. In the case of total knee arthroplasty, different contact surface can be due to different surgical techniques, namely resurface and non-resurface patella. In the resurface patella technique, patellar cartilage will be replaced by the prosthesis. For non-resurface patellar technique, the patella is intact. VAG signals from resurface class are basically from the moving contact of polyethylene and titanium, whereas signals of the non-resurface class are from the natural patellar cartilage and titanium. Decision to perform either resurface or non-resurface patellar is based on individual physician [NASK00]. In terms of VAG signal, as different contact surface could alter the signal, we hypothesized that VAG signals of resurface and non-resurface classes should be different. The aim of this study was therefore to study and classify the VAG signals from these two classes.

# 2 Overview on time-domain VAG signals

This section provide the description of VAG signals and the procedure of data acquisition.

## 2.1 Measurement and assumption on VAG Signals

In a measurement process, subjects sitting on a chair were assisted to perform a leg extension (0 degree) and flexion (90 degree). During an assistance, subject's leg is fully relaxed resulting in less noise from muscle contraction. A piezoelectric accelerometer is attached on subject's knee cap corresponding to the mid-patella position of the knee, as shown in 1. Subjects were asked to sit on the flat surface with legs suspending in the air. Before the measurement, the subjects were rested for 5 minutes. This is because a prior movement in knee causes VAG signals to become *smoother* [BE02]. However, after 5 minutes of rest, the knee will return to its initial condition [MMB+87].

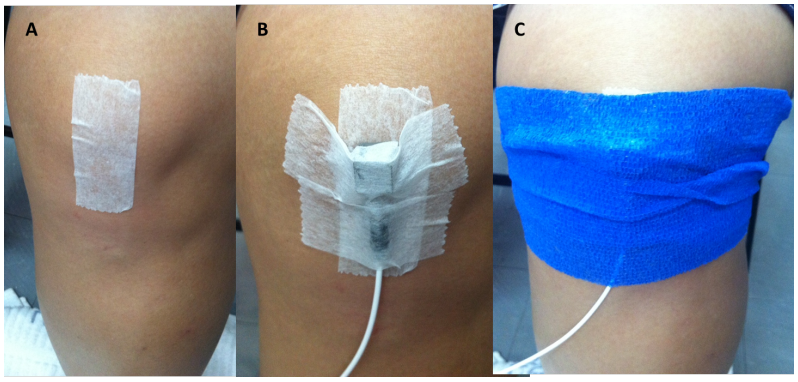


Figure 1: The position of an accelerometer attachment.

The subjects were assisted to extend and flex their legs. An assistance to the subject movement is required to control the frequency of each cycle. Suppose that the line parallel to subject lap is 0°, one cycle contains movement from 0° to 90° and back to 0°. An iteration of measurement approximately contains $9 - 15$ cycles.

The raw VAG signals of 10 patients were recorded by the PCB accelerometer model 333B32 with sampling frequency at 12.8 kHz and by using the vibration analyzer (OR36, 16-channel, Teamwork Multianalyzer Recorder, OROS). The description of patients is given in the Table 1.

Table 1: Additional subject description of the non-resurface and resurface classes. In the side column, L and R indicate left and right knee; and in the condition column R and N indicate resurface and non-resurface class respectively. The data are 10 subjects with 14 conditions. Some subjects were performed in several trials and this results in 30 different data sets.

| Subject | Gender | Age | Side | Condition | Time after surgury |
|---|---|---|---|---|---|
| 1 | F | N/A | L | R | 6 Y |
| 2 | F | N/A | R | N/A | N/A |
| 3 | M | N/A | R | N | 3 M |
| 4 | F | 70 | R | N | N/A |
| 5 | F | 73 | R | N | N/A |
| 6 | F | 66 | L | N | N/A |
| | | | R | N | 1 Y |
| 7 | F | 68 | L | N | 2 Y |
| | | | R | R | 3 Y |
| 8 | M | N/A | R | N | 6 M |
| 9 | F | 69 | L | R | 10 Y |
| | | | R | R | 10 Y |
| 10 | F | N/A | L | R | 7 Y |
| | | | R | R | 7 Y |

## 2.2 Resurface and non-resurface VAG signals

The non-resurface and resurface VAG signals are plotted in Figure 2a and Figure 2b respectively. In the figure titles, S denotes subject, L denotes VAG signal from left knee and R denotes VAG signal from right knee, a number after L and R is a number of iteration performed in measurement process. The magnitudes of all subject's range between $-5$ and $5\,m/s^2$. From the figures, we can read that the low frequency components from motion of the knee is around $f = 0.4$ Hz. This frequency of rotation is controlled while performing a knee measurement, *i.e.*, a subject is asked to rotate their knee approximately within 2 seconds. At the beginning and end of revolution, VAG signals are noisy as [LLWW12] suggests. A spike in VAG signal is suspected to be a result of implosion of bubble in synovial fluid causing a slip-stick vibration.

From our hypothesis, non-resurface VAG signal should have more high frequency components. In contrast to our hypothesis, some of resurface VAG signals (Patella replacement with smooth materials) such as from `S9 L1, S9 R1, S7 R1` seem to have more high frequency components. In other word, non-resurface VAG signals are *smoother*. However, from Figure 2c, we observe that VAG signals from non-resurface subject 6, when measuring under lay self condition, has significant high magnitude, which is about $100\,m/s^2$, 20 times higher than normal range; see Figure 2e. Besides, results from subjects with sounds in Figure 2d are not different from the other classes. Although there is no significant differences between resurface and non-resurface class, magnitude of VAG signals seem to depend on sound heard during measurement. In the Figure 2c, VAG signals from subject 6 has higher magnitude than subject 1 and 4, of which quieter sound are heard.

## 2.3 VAG signals of swine knee joint

The availability of VAG signals from patients is typically limited and up to the number of follow-up patients in the hospital. And we have to be certain that the signal we obtained is really from deterioration of the cartilage not from the movement of other soft tissues in the knee joint. Another direction of our on-going work is therefore to develop and improve a device that simulates the knee joint movement so that we can take the signal and test the hypothesis that different articular cartilage surface roughness should give different vibration signal. We have modified a machine that can provide the periodic translational relative motion of the two moving surfaces, i.e. the articular surfaces of patella and femoral condyle of the swine knee joint, as illustrated in Figure 3. The machine is basically composed of a motor, in which the power is transmitted through the

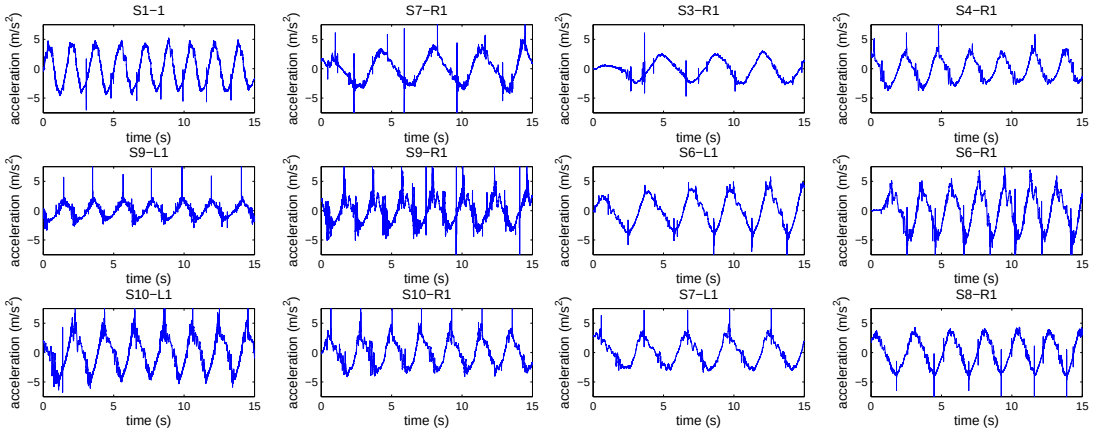


(a) Resurface (b) Non-resurface

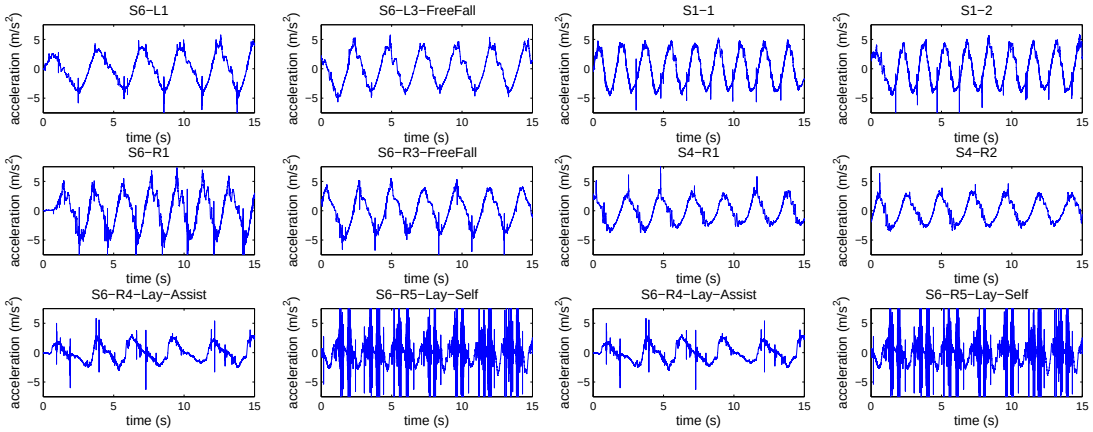


(c) Subject 6 under different conditions (d) Subjects with sound

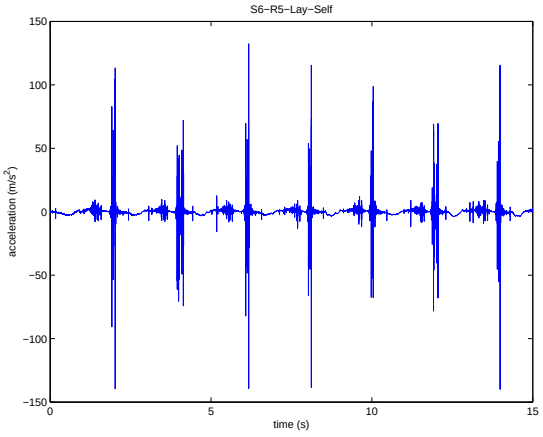


(e) Subject 6 has high-amplitude signal

Figure 2: Time-domain VAG signals of subject 6 measured in various conditions. The horizontal axis is time (s) and vertical axis is the acceleration ($m/s^2$).

shaft, pulley, gear box and finally the cam to generate the periodic translational motion. Special jig and fixture has to be redesigned so that the swine bones can be held; see Figure 3b.

Typically during walking, the knee joint rotation angle is between 0° to 15° in which the motion of the patella and femoral condyle is relatively in translation. So the swine patella and femoral condyle bones are cut to fit the jig and fixture of the machine (see Figure 3b) and used to simulate the relative translational motion with the distance of 1.5 cm and period of 1.392 seconds. In this

way, we can simulate the knee joint movement with different swine's knee cartilage deterioration model.

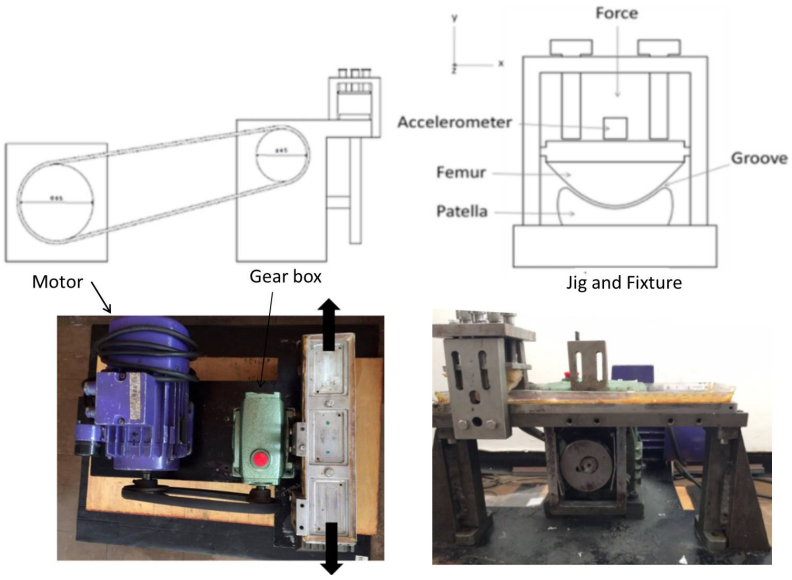


(a) A development of device that simulates swine knee joint movements.

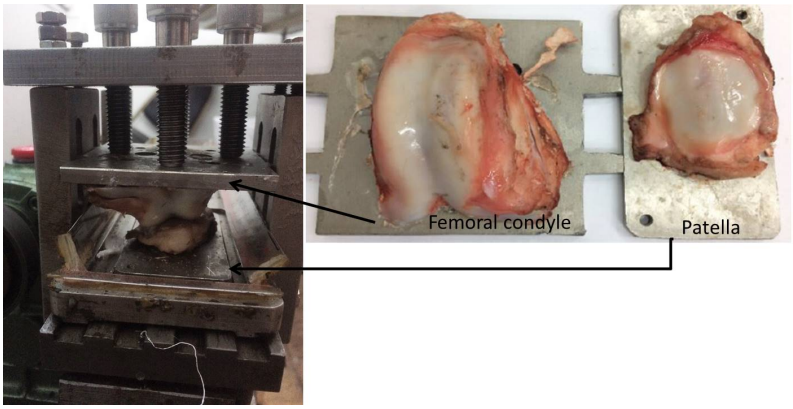


(b) The measurement of swine knee joint rotation.

Figure 3: An experiment set up for measuring swin knee joint data.

Our analysis part will not involve with the swine knee data from this experiment.

# 3 Methodology

The VAG signals of 10 subjects are collected from the measurement process. Similar to other physiological signals, VAG signals collected are contaminated by noise, for example, from muscle contraction [BE02]. Besides, there also components that are irrelevant to the characteristics of VAG signal such as motion trend. For these reasons, they are subject to be pre-processed in order to remove motion trend and noise. The processed signals will then be analyzed by frequency-domain tools, the short-time Fourier transform. In this section, we provide a brief description of signal processing tools used in this study.

## 3.1 Time-Domain Signal Processing

Raw VAG signals can contain some artifacts, random noise and baseline wander which are supposed to be removed before analyzing the intrinsic characteristics of the signals. Firstly, a *baseline*

*wander* which is a slowly moving trend is removed by applying a high pass filter. Secondly, the random noise is removed by the technique of *ensemble empirical model decomposition (EEMD)* and *detrended fluctuation analysis (DFA)* [KKBR$^+$01]. We consider this approach because the EEMD technique was introduced [HZL$^+$98, Sch01] for analyzing time series generated from nonlinear and non-stationary processes. This characteristics are observed in VAG signals where statistical properties of the processes change over time. The EEMD method decomposes a signal into a series of the so-called *intrinsic model functions (IMFs)* that represent an embedded characteristic oscillation on a separated time-scale. Suppose that EEMD decomposes the signal into $n$ mode, the signal $x(t)$ and $k^{\text{th}}$ IMFs, denoted by $c_k$, has the relation given by

$$x(t) = \sum_{k=1}^{n} c_k(t) + r_n,$$

where $r_n$ is the residual. Lastly, from the IMFs decomposed by EEMD, we determine if each IMF contains represents noise characteristic or artifacts in the signal. A dominant feature of noise is its short-range correlated property (noise occured at short period of consecutive times are almost uncorrelated.) Therefore, a technique called Detrended Fluctuation Analysis (DFA) can then be applied to analyze such correlation property of each IMF. The idea of this technique can be explained briefly as follows [PHSG95]. Firstly, consider the correlation function

$$C(s) = \mathbf{E}[x(t)x(t+s)] \approx \frac{1}{N-s} \sum_{t=1}^{N-s} x(t)x(t+s)$$

where $x(t)$ is zero-mean signal. The method suggests that if $x$ has a *long-range* correlation then $C(s)$ should obey a power law: $C(s) \propto s^{-\gamma}$ where $0 < \gamma < 1$ and our goal is to determine $\gamma$, the correlation exponent, *indirectly* via the computation of a *fluctuation function*. This function, denoted by $F(s)$, is obtained by dividing the signal into parts of sample size $s$, removing a polynomial trend, and then computing its variance. The detail of these steps are provided in DFA algorithm [KKBR$^+$01]. Once, the fluctuation function is computed, the relation between the correlation of the signal $x(t)$ and $F(s)$ is stated as follows.

- If the signal is long-range power-law as $C(s) \propto s^{-\gamma}$, then the fluctuation function increases by a power law $F(s) \sim s^{1-\gamma/2} \triangleq s^{\alpha}$, where $\alpha = 1 - \gamma/2$ for $0 < \gamma < 1$.
- If the signal is uncorrelated or short-range correlated then $F(s) \sim s^{1/2}$ (see the detail of this claim in [KKBR$^+$01]), *i.e.*, $\alpha = 1/2$ indicates short-range correlation of the signal. For example, if the signal is white noise, its fluctuation exponent should be $\alpha = 1/2$.

In DFA procedure, we calculate $\alpha$ of each IMF and discard the IMFs associated with $\alpha \leq 0.5$ and reconstruct the VAG signal from the remaining IMFs. The IMFs which show randomness should be discarded before being composed back.

## 3.2 Short-Time Fourier Transform

From section 2, VAG signals are suspected to be non-stationary. More than one iteration of knee movement is needed to study the knee condition of each subject. A power spectral density (PSD) or other straightforward frequency analysis might be misleading because if a sign of abnormal knee is presented inconsistently, its magnitude will be averaged by the whole signal, which can be misunderstood to be a noise. There is an attempt to decompose VAG signals into the sum of stationary signals, which provides a way to study VAG signals with stationary methods [TRF$^+$92]. In this section, we employ a similar and time-dependency method called *short time Fourier transform (STFT)* [OSB99] where signals are pre-windowed in a particular instant in time and calculate its Fourier transform, assuming the signals to be stationary in all windows. Thus, it is possible to observe changes in frequency characteristics as the knee rotates at each position. However, in order to get a high frequency resolution, one needs to increase the window width (longer time spans), while in order to specify an event in time, the window width should be narrow. Thus, the window width must be choosen appropriately. Such window is chosen to be a function, so that

a part of VAG signals taken into the window is weighed. In each iteration, the window is moved 25% of the window length to analyze the next part of a VAG signals.

In conclusion, a processing pipeline is introduced in Figure 4 to filter out the motion trend and extract the spikes. We then apply EEMD to decompose the original VAG signals into different modes (IMFs) and apply DFA algorithm to check the correlation of each IMF. We choose the criterion $\alpha \leq 0.5$ to discard uncorrelated IMFs. Finally, the set of IMFs that pass the criterion will be composed back to be the processed signal $x_{\text{processed}}$. The EEMD and DFA technique together can efficiently remove artifacts in VAG signals [WYZ+14]. Since spikes account for large portion of VAG signal energy and are considered to be one of the characteristics, we propose a spike extraction block that preserve spikes before the signal undergoes the EEMD block. Additionally spike extraction make each IMFs easier to be observed. In order to analyze processed VAG signal, STFT (Short Time Fourier Transform) is used. With STFT, information are obtained in both time and frequency so that it is possible to observe frequency and change of frequency in each flexion-extension cycle.

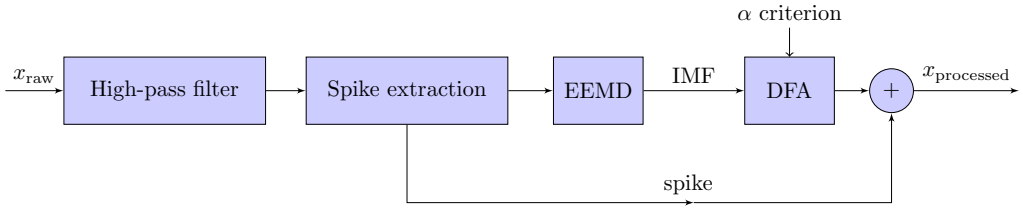


Figure 4: VAG signal processing pipeline.

### 3.3 Features of VAG signals

Let $\{x(t)\}_{t=1}^{N}$ be the time-domain and $X(\omega)$ be the frequency-domain (spectrum) signals, respectively. The author in [BM14] used the following features to assess the VAG signals.

1. *Variance over the entire duration (VMS).* Suppose $x(t)$ is partitioned into non-overlapping $K$ segments of 5 ms each; $x(t) = (x_1(t), x_2(t), \ldots, x_K(t))$. Denote $\text{MS}_k$ a mean-squared value of $x_k(t)$ and computed by $\text{MS}_k = (1/L)\sum_t x_k(t)^2$ where $L$ is the length of $x_k(t)$ in each segment. The average of mean-squared values from $K$ segments is denoted as $\overline{\text{MS}}$. VMS is therefore defined as the variance of the mean-squared values:

$$\text{VMS} = \frac{\sum_{k=1}^{K}(\text{MS}_k - \overline{\text{MS}})^2}{(K-1)}.$$

2. *Amplitude range.* Suppose $x(t)$ is the VAG signal after a motion trend has a period of $T$ and contains $K$ full cycles. We calculate the amplitude range of VAG signals as the average of the difference between maximum and minimum values in one period.

$$\text{R}_\text{K} = \frac{1}{K}\sum_{k=1}^{K}\left(\max_{t\in[0,T]} x(t) - \min_{t\in[0,T]} x(t)\right).$$

   This feature is denoted as R4 in [BM14] as there were 4 full cycles in their experiment.

3. *Spectral power in P1 band.* We can perform a short-time Fourier transform analysis by computing discrete Fourier transform of windowed VAG signals. The power spectrum is analyzed by integrating the power density over a frequency band of interest. In this case, P1 band is the interval of $50 - 250$ Hz.

4. *Spectral power in P2 band.* Similarly, this is the spectral power in $250 - 450$ Hz.

In [BM14], the above features were calcuated from VAG signals of four classes of patients: i) control, ii) chondromalacia, iii) with lateral compression syndrome, and iv) with osteoarthritis. Their results show that normal patients have low values of VMS and R4 and have low power in both P1 and P2 bands. Patients with osteoarthritis, on the other hand, has large VMS and R4, and have high spectral power in P1 band.

### 3.4 VAG signals from the simulation of swine knee joint

The motion simulation machine (Figure 3b) is used to simulate the movement of the knee joint similar to walking, *i.e.*, the patella motion over the femoral condyle is in translation of 1.5cm distance with the period of 1.392 seconds. Enzyme collagenase is used to deteriorate the articular cartilage, making it an early grade damage, before putting the cut bones in the fixture of the machine. As the machine is running, the early grade damaged patella is rubbing constantly over the cartilage of femoral condyle. VAG signals are taken during the running of the machine until the cartilage is completely damaged. In this way, VAG signal during cargilate degeneration progression can be obtained and analyzed.

## 4 Experimental results

The experimental results in this section contains three parts: 1) the results on pre-processing signals in time-domain 2) the short-time Fourier analysis results and 3) the results on the special cases. The experiments are based on using the human knee joint data only.

### 4.1 Pre-processing of VAG signals

Plots of VAG signals of non-resurface and resurface classes are shown in Figure 5. VAG signals contain three main components as follows: (i) Acceleration from motion which will be called *motion trend* through out this paper. The simplest model of such motion is described by sinusoidal function. (ii) Micro vibration from inner structure of knee joint. Such vibrations are generated from articular cartilage surfaces of Femur (thigh bone), Patella, and Tibia (shin bone) rubbing to each other. (iii) Spikes which are the high magnitude components occurring periodically at the either beginning or end of the flexion-extension cycle. Spikes are supposed to be either the results of implosion of bubble in synovial fluid causing a slip-stick vibration or snapping tendon.

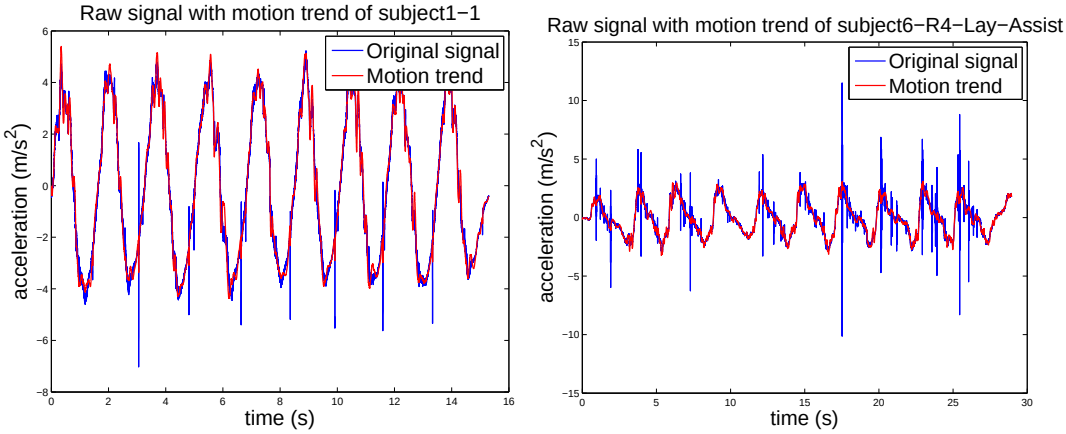


(a) Resurface (b) Non-resurface

Figure 5: Example of original signal is in blue and the motion trend is in red.

After being processed according to the proposed pipeline in Figure 4, the processed signals are plotted in Figure 6. The two time-domain features; VMS and the amplitude range explained in Section 3.3 are calculated and plotted in Figure 7. It appears that the data plots from two classes of patients cannot be visually distinguished by a simple linear classifier.

### 4.2 Frequency-domain analysis of VAG signals

Time-frequency plots (spectrograms) of non-resurface and resurface VAG signal are shown in Figure 8. From time results in Figure 6 and time-frequency results in Figure 8, there is no distinct feature to separate the non-resurface and resurface groups from each other. Since the hypothesis

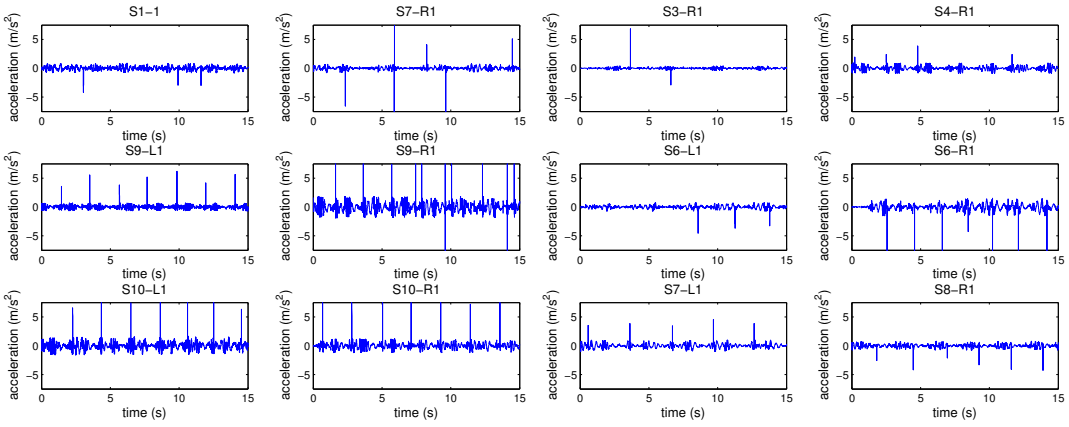


(a) Resurface (b) Non-resurface

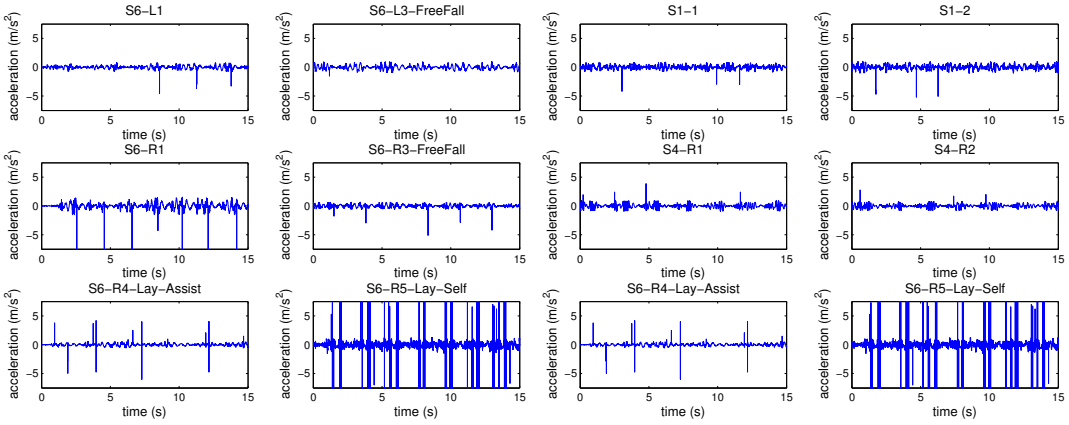


(c) Subject 6 under different conditions (d) Subjects with sound

Figure 6: Time-domain result of processed signals

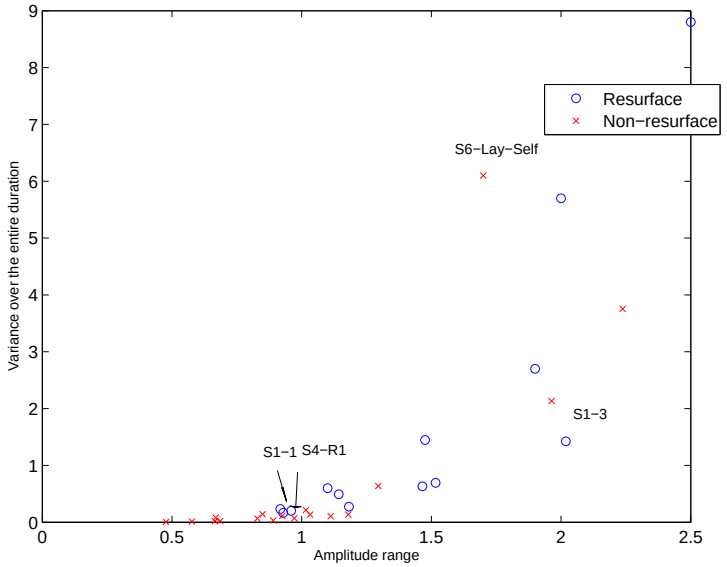


Figure 7: Time-domain features of VAG signals from two groups of patients.

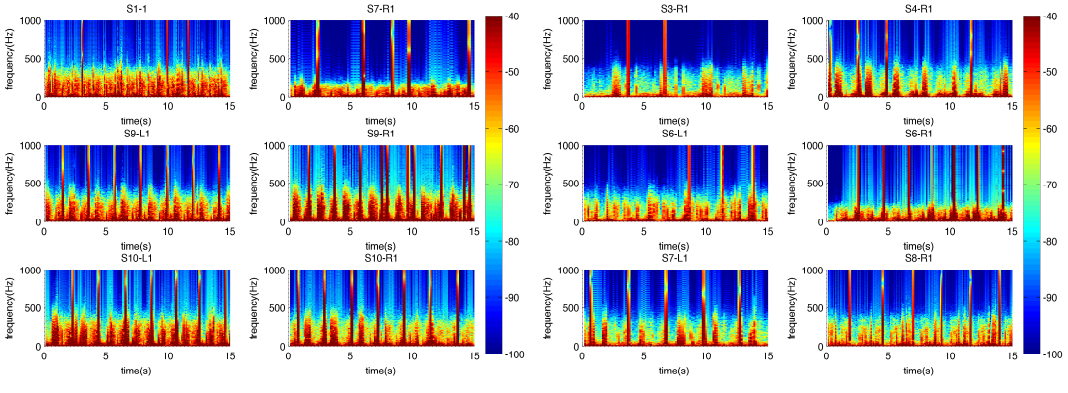


(a) Resurface (b) Non-resurface

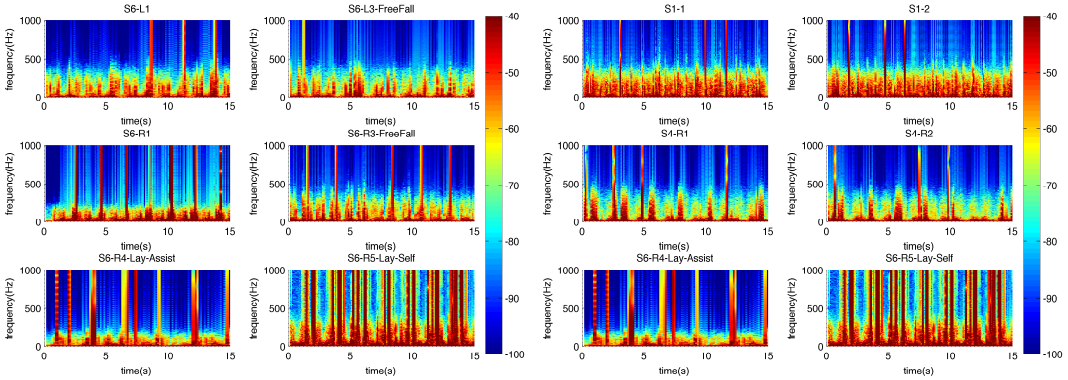


(c) Subject 6 under different conditions (d) Subjects with crepitus

Figure 8: STFT results of processed signals

is that VAG signal are different in mid-range frequency, two band of mid-range freqency P1 and P2 are chosen to compare numerically. If considering range used in the literature, band P1 (50-250 Hz) and P2 (250-450 Hz), normalized by signal length, are calculated from all 30 data sets as shown in Table 2. Despite that P1 and P2 from resurface and non-resurface class are different in mean value, standard deviation are too high to classify with P1,P2. Such ambiguity in classification is illustrated by Figure 9.

Table 2: Frequency band power comparison between resurface and non-resurface class

| | P1 (50-250 Hz) (W) | P2 (250-450 Hz) (W) |
|---|---|---|
| Resurface | $(3.9252 \pm 2.6928) \times 10^4$ | $52.2507 \pm 51.2711$ |
| Non-resurface | $(2.1963 \pm 1.4726) \times 10^4$ | $19.6485 \pm 17.3809$ |

## 4.3 Discussion

In this section, we discuss the results of analyzing VAG signals as follows.

1. Variation on the measuring condition: Consider an interesting result of subject 6 whose VAG signals were measured in various condition labeled by `S6 R1, S6 R3 Freefall, S6 R4 Lay Assist` with description:

   - Freefall: Subject was sitting on a chair, moving the knee up and let it fall down freely to the original position.
   - Lay Assist: Subject was lying on a bed and moved the knee up with assistance.
   - Lay Self: Subject was lying on a bed and moved the knee up by him/herself.

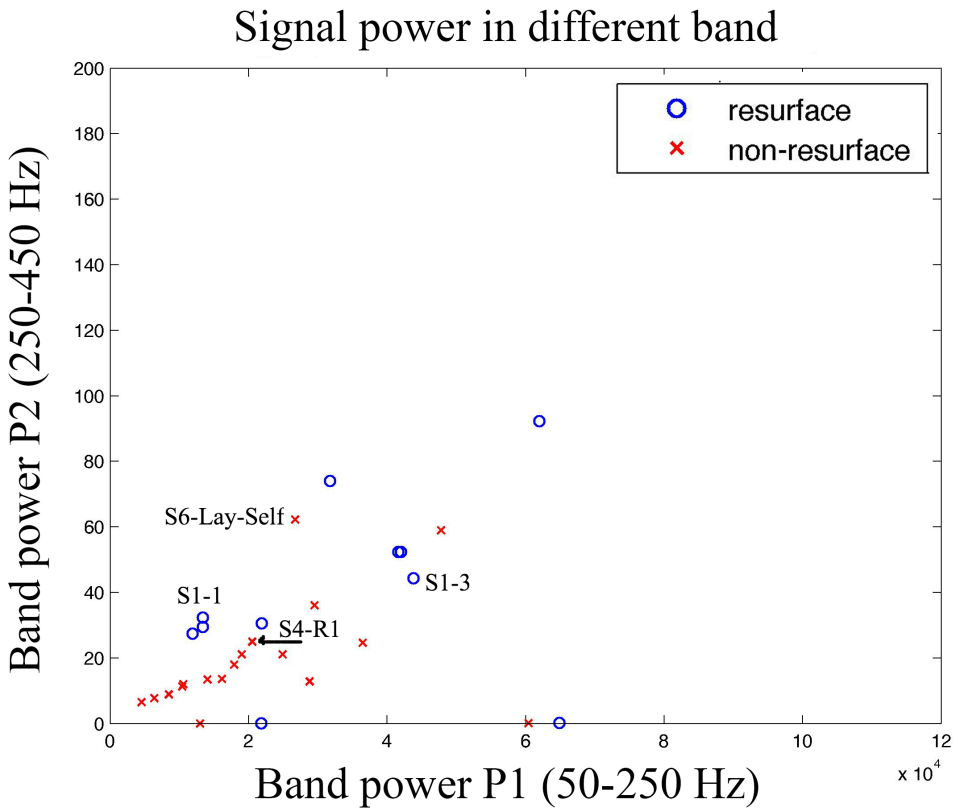


Figure 9: From all data sets, resurface and non-resurface class are plotted according to their P1 and P2 properties. Obviously, there are no differences or even a cluster of data.

During the measurement process, the physician heard *crepitus* sound which is an indication of degraded knee as the subject was lying on a bed (`Lay Self`). From result in `S6 R4 Lay Assist` and `S6 R5 Lay Self` in Figure 6 (c) and Figure 8 (c), the position of lying down on the bed would not affect the measurement results. Although VAG signals of `S6 R1`, `S6 R3 Freefall`, `S6 R4 Lay Assist` and `S6 R5 Lay Self` are from subject 6's right knee, physician only heard crepitus sound under Lay Self condition.

2. Results from patients with knee sound: Since there are no differences between resurface and non-resurface class, we hypothesize that the feature characteristics of the signal should depend upon individual and one's knee condition. Thus, the results from subject 1,4,6 which physician heard the cracking sound are chosen for a comparison. We hypothesize that if physician can observe the degradation in knee, VAG signal will show a considerable magnitude of the characteristic frequency. The result in Figure 8 (d) agree with this hypothesis since subject 6's crepitus sound were heard while subject 1 and 4 only produce cracking and gob-gab sound. Despite no significant difference time-frequency results between subject with sound and other class, *i.e.*, Figure 8 (d) and Figure 8 (a), 8 (b) and 8 (c), power of signals of this type is higher than the other class especially from subject 6, $3.64 \times 10^4$, which is the highest and about one standard deviation higher than the average of $2.89 \times 10^4$. A

3. Subject 6,7,9, and 10 are the patients who have gone knee replacement on both knees. All of them had the same option of resurface replacement except the subject 7 who had resurface replacement on the right knee but non-resurface on the left knee. The STFT plot in Figure 8 (a) and (b) show that the non-resurfaced knee signal (of subject 7) has more power in P2 band than the resurfaced knee signal, while the resurfaced knee signals of both knees have similar amount of power in P2 band in subject 9 and 10. There is no clear conclusion from these cases whether the classification performance (in terms of signal power) should depend on the resurface option or subject rather than the knee condition.

# 5 Conclusion and future work

In conclusion, VAG signal of class resurface and non-resurface are studied to find their differences and similarities. Since raw VAG signals contain baseline wander and random noise, the signals should be processed before analysing. Signal processing technique is introduced to eliminate such artifacts as follow: (i) baseline wander is removed by high-pass filter. (ii) random noise is removed by EEMD/DFA. The signal is first decomposed with EEMD, non-stationary signal processing technique to obtain a set of IMFs. Then each IMFs is analysed with DFA to obtain their correlation properties in term of $\alpha$. After that IMFs having $\alpha \leq 0.5$ are discarded. Finally, the processed signal is analysed in time-frequency domain to observe its time-frequency characteristics. Differences of time-frequency results under different measurement condition are observed. Contary to the hypothesis, only one subjects with cracking sounds has a distinct time-frequency result. Nevertheless, there is no clear distinction results between non-resurface and resurface class both in time and time-frequency domain.

As there are different other tissue structures that can contribute to the VAG signals, the obtained VAG signals could be from other conditions, not just the difference in the contact articular surfaces. One observation of the VAG signal was the consistency of the signals in each individual. VAG signals from the same knee under the same recording condition looked similar for all moving cycles, but different from subject to subject. Future study would be to examine how different structures and conditions contribute to the VAG signals. Additional clinical information of each subject, such as medical imaging like MRI, may be helpful.

In order to apply some statistical learning techniques to analyze knee data, it requires more number of data samples, regardless of the choice of supervised, or unsupervised learning techniques. Another limitation of our work is that we solely rely on the availability of follow-up patients in the collaborator's hospital. The motion simulation machine that is used with swine knee joint can provide a substitute and allow us to analyze the instrinsic properties of knee joints in our future research.

# 6 Appendix

In this section, we provide the detailed results of all subjects both in time and frequency domains. Details of EMD and DFA algorithms are also presented.

## 6.1 Butterworth Highpass filter

We choose Butterworth IIR high-pass filter of order 2 to filter the baseline wander. The filter is designed with specification: $A_{\text{stop}} = -80dB, A_{\text{pass}} = 1dB, f_{\text{top}} = 1, f_{\text{pass}} = 2$. The filter is designed by the `fdatools` toolbox in MATLAB (a scientific computing software) and has the transfer function described by $|H(j\omega)|^2 = (1 + (\frac{\omega}{\omega_{\text{cutoff}}})^4)^{-1}$.

## 6.2 Empirical Mode Decomposition (EMD)

This technique is based on an assumption that a signal at any given time may contain many oscillatory modes of different frequencies. The method decomposes the signal into several components called *intrinsic mode function (IMF)* which satisfies the following two conditions:

1. the number of extrema and the number of zero crossing must either be equal or differ at most by one;
2. at any time point, the mean value of the envelope defined using the local maxima and the envelope defined using the local minima is zero.

The decomposition can be done through a *sifting process* which can be described as follows. Let $x(t)$ be an arbitrary raw signal fed to this process.

1. Identify maxima and minima of $x(t)$.
2. Connect all the local maxima (and minima) by a cubic spline line. This forms the upper and lower envelopes and the signal $x(t)$ lies between these two envelopes.
3. Calculate the mean between the two envelopes, denoted by $m_1$ and define $h_1 = x(t) - m_1$ as the first protomode.
4. We expect that $h_1$ to satisfy the properties of the IMF but it generally does not, so we repeat the process of fitting the cubic spline where in the next iteration we treat $h_1$ as the new input. Hence, we repeat

$$\begin{aligned} h_{11} &= h_1 - m_{11} \\ h_{12} &= h_{11} - m_{12} \\ \vdots &\quad \vdots \\ h_{1k} &= h_{1(k-1)} - m_{1k} \end{aligned}$$

   until the condition on the local envelope symmetry of the IMF function is satisfied, *i.e.*, $h_{1k}$ becomes the IMF function and defined as $c_1$;

$$c_1 = h_{1k}$$

   which is the first IMF component. Several stopping criterions in the sifting process have been proposed [HW08] such as a small relative change in $h_k(t)$ or a small sum-squared amplitude of $m_{1k}$.

Once the first IMF is obtained, which should contain the shortest-period oscillation, we compute the residual

$$r_1 = x(t) - c_1$$

which still consists of longer-period oscillations. This residual is then treated as the *new data* and applied to the sifting process again and obtain the second IMF, $c_2$. We repeat this process to obtain the residuals:

$$\begin{aligned} r_2 &= r_1 - c_2 \\ r_3 &= r_2 - c_3 \\ \vdots & \quad \vdots \\ r_n &= r_{n-1} - c_n \end{aligned}$$

and stop when the residual of the $n$th iteration becomes a monotonic function where no more IMF can be extracted. As a result, the original signal can be written as

$$x(t) = \sum_{k=1}^{n} c_k(t) + r_n$$

where $x(t)$ can be decomposed as $n$ IMFs with a residual $r_n$. We note that in EMD method, removing a constant mean from the input signal is not required since the zero reference is calculated during the sifting process.

## 6.3 Ensemble Empirical Mode Decomposition (EEMD)

It is not common that EMD is implemented alone but rather carried out through the standard technique called EEMD. EEMD technique is introduced to overcome mode mixing and improve the stability of EMD technique [HZL+98]. Literally, EEMD implement EMD for $N$ iteration. The process is explained in steps followed:

1. Mixing with white noise: Raw input signal $x(t)$ is mixed with white noise to become input signal of $k^{\text{th}}$ iteration
$$x_k(t) = x(t) + w(t),$$
where $w(t) \sim \mathcal{N}(0, 1)$. The magnitude of white noise is normally chosen to be one standard deviation of the input signal.

2. EMD subroutine: The input signal of $k^{\text{th}}$ iteration $x_k(t)$ is applied with EMD technique yielding a set of IMF of $k^{\text{th}}$ iteration $\{c_{k,1}, c_{k,2}, c_{k,3}, \ldots, c_{k,n}\}$.

3. Average signal from all iteration: The IMF resulting from each iteration are averaged to obtain the single IMF result. For example IMF#1 is evaluated by $c_1 = \sum_{k=1}^{N} c_{k,1}$. By averaging the white noise added in first step is assumed to cancle out each other.

In spite of repetitions, EEMD can be efficiently implemented by C/C++ library that supported multithreading [LHR15]. As default configuration, the number of iteration $N$ is chosen to be 250 and the number of sifting process is limited to 10.

## 6.4 Detrended Fluctuation Analysis (DFA)

DFA is a method for detecting autocorrelation in time series with non-stationary property [KKBR+01, PHSG95]. It determines how correlated a signal is and measures this property in terms of a scalar parameter, $\alpha$. The idea of this technique can be explained briefly as follows. Firstly, consider the correlation function

$$C(s) = \mathbf{E}[x(t)x(t+s)] \approx \frac{1}{N-s} \sum_{t=1}^{N-s} x(t)x(t+s)$$

where $x(t)$ is zero-mean signal. The method suggests that if $x$ has a *long-range* correlation then $C(s)$ should obey a power law:

$$C(s) \propto s^{-\gamma} \tag{1}$$

where $0 < \gamma < 1$ and our goal is to determine $\gamma$, the correlation exponent, *indirectly* via the computation of a *fluctuation function*. This function, denoted by $F(s)$, is obtained by dividing

the signal into parts of size $s$, removing a polynomial trend, and then computing its variance. The paper [KKBR$^+$01] states that:

- If the signal is long-range power-law as in (1), then the fluctuation function increases by a power law
$$F(s) \sim s^{1-\gamma/2} \quad \triangleq \quad s^{\alpha}.$$
where $\alpha = 1 - \gamma/2$ for $0 < \gamma < 1$,
- If the signal is uncorrelated or short-range correlated then $F(s) \sim s^{1/2}$ (see the detail of this claim in [KKBR$^+$01]), *i.e.*, $\alpha = 1/2$ indicates short-range correlation of the signal. For example, if the signal is white noise, its fluctuation exponent should be $\alpha = 1/2$.

In practice, we will calculate $F(s)$ from the DFA algorithm, determine the fluctuation exponent $\alpha$ and make a conclusion about the correlation property of this value. We now describe the DFA algorithm. Consider a time series $x(t)$ for $t = 1, 2, \ldots, N$ and its mean defined by $\bar{x} = (1/N)\sum_{t=1}^{N} x(t)$.

1. We integrate the time series $x(t)$.
$$y(t) = \sum_{k=1}^{t} [x(k) - \bar{x}],$$
and $y$ is called the integrated time series.
2. The integrated time series is divided into boxes of equal length, $s$. In each box of length $s$, we perform a least-squares polynomial fit, called a *local trend*, to $y$. Let $y(i)$ denote the $i$th chunk of $y$ where $i = 1, 2, \ldots, \text{floor}(N/s)$. Therefore, the detrended time series is given by
$$Y(i) = y(i) - p(i), \quad i = 1, 2, \ldots, \text{floor}(N/s),$$
where $p(i)$ is the fitted polynomial (local trend) to the data in the $i$th chunk. The local trend can be choosen to be a fixed order of polynomial.
3. We compute the root-mean-square fluctuation of this integrated and detrended tiem series, called the *fluctuation function*:
$$F(s) = \sqrt{\frac{1}{N}\sum_{k=1}^{N} (Y(t))^2}.$$
4. Repeat the steps 2)-3) over all time scale $s$. It is shown that $F(s)$ will increase as the length of time scale, $s$, increases. We can plot $\log F(s)$ versus $\log s$ to see if the fluctuation function obeys a power law: $F(s) \propto s^{\alpha}$.

The interpretation of the correlation exponent, $\alpha$, can be summarized according to [PHSG95] below.

- $0 < \alpha < 0.5$: the signal is correlated but large and small values are likely to alternate.
- $\alpha = 0.5$: white noise.
- $0.5 < \alpha < 1$: the signal has a long-range correlation.
- $\alpha = 1$: $1/f$ noise (or pink noise).
- $\alpha > 1$: the signal has a correlation explained by the power law.
- $\alpha = 1.5$: brown noise (integration of white noise).

# References


[BE02] Blodgett and Willium Ernest. Auscultation of the knee joint. *The Boston Medical and Surgical Journal*, 146(3):63–66, 1902.

[BM14] Dawid Baczkowicz and Edyta Majorczyk. Joint motion quality in vibroacoustic signal analysis for patients with patellofemoral joint disorders. *BMC musculoskeletal disorders*, 15(1):426, 2014.

[CGZ78] M.L. Chu, I.A. Gradisar, and L.D. Zavodney. Possible clinical application of a noninvasive monitoring technique of cartilage damage in pathological knee joints. *Journal of Clinical Engineering*, 3(1):19–27, 1978.

[HW08] N.E. Huang and Z. Wu. A Review on Hilbert-Huang transform: Method and its applications to geophysical studies. *Reviews of Geophysics*, 46(2), 2008.

[HZL+98] N.E. Huang, S. Zheng, S.R. Long, M.C. Wu, H.H. Shih, Q. Zheng, N. Yen, C.C. Tung, and H.H. Liu. The Empirical mode decomposition and the Hilbert spectrum for nonlinear and non-stationary time series analysis. *Proceedings of the Royal Society of London A: Mathematical, Physical and Engineering Sciences*, 454(1971):903–995, 1998.

[KKBR+01] J.W. Kantelhardt, E. Koscielny-Bunde, H. Rego, S. Havlin, and A. Bunde. Detecting long-range correlations with detrended fluctuation analysis. *Physica A: Statistical Mechanics and its Applications*, 295(3):441–454, 2001.

[LHR15] P. J. J. Luukko, J. Helske, and E. Räsänen. Introducing libeemd: a program package for performing the ensemble empirical mode decomposition. *Computational Statistics*, 31(2):545–557, 2015.

[LLL+14] W.C. Lin, T.F. Lee, S.Y. Lin, L.F. Wu, H.Y. Wang, L.W. Chang, J.M. Wu, J.C. Jiang, C.C. Tuan, M.F. Horng, C.S. Shieh, and P.J. Chao. Non-invasive knee osteoarthritis diagnosis via vibroarthrographic signal analysis. *Journal of Information Hiding and Multimedia Signal Processing*, 5(3):497–507, 2014.

[LLWW12] Tsair-Fwu Lee, Wei-Chun Lin, Li-Fu Wu, and Hung-Yu Wang. Analysis of vibroarthrographic signals for knee osteoarthritis diagnosis. In *Genetic and Evolutionary Computing (ICGEC), 2012 Sixth International Conference on*, pages 223–228, Aug 2012.

[MMB+87] GF McCoy, JD McCrea, DE Beverland, WG Kernohan, and RA Mollan. Vibration arthrography as a diagnostic aid in diseases of the knee. a preliminary report. *The bone and joint journal*, 69-B:288–293, MarcZFRB:92h 1987.

[NASK00] J.H. Newman, C.E. Ackroyd, N.A. Shah, and T. Karachalios. Should the patella be resurfaced during total knee replacement? *The Knee*, 7(1):17–23, 2000.

[OSB99] Alan V. Oppenheim, Ronal W. Schaffer, and John R. Buck. *Discrete Time Signal Processing*. Prentice-Hall, Upper Saddle River, New Jersey, 2 edition, 1999.

[PHSG95] C.-K. Peng, S. Havlin, H. Eugene Stanley, and Ary L. Goldberger. Quantification of scaling exponents and crossover phenomena in nonstationary heartbeat time series. *Chaos: An Interdisciplinary Journal of Nonlinear Science*, 5(1):82–87, 1995.

[Sch01] T. Schlurmann. The Empirical mode decomposition and the Hilbert spectra to analyse embedded characteristic oscillations of extreme waves. In *Rogue Waves 2000 (Workshop organized by IFREMER)*, pages 157–165, 2001.

[TRF+92] S. Tavathia, R.M. Rangayyan, Cyril Basil Frank, G.D. Bell, K.O. Ladly, and Y.-T. Zhang. Analysis of knee vibration signals using linear prediction. *Biomedical Engineering, IEEE Transactions on*, 39(9):959–970, Sept 1992.

[WKR10] Y. Wu, S. Krishnan, and R.M. Rangayyan. Computer-aided diagnosis of knee-joint disorders via vibroarthrographic signal analysis: a review. *Critical Reviews in Biomedical Engineering*, 38(2), 2010.

[WYZ+14] Y. Wu, S. Yang, F. Zheng, S. Cai, M. Lu, and M. Wu. Removal of artifacts in knee joint vibroarthrographic signals using ensemble empirical mode decomposition and detrended fluctuation analysis. *Physiological measurement*, 35(3):429, 2014.